Chapter 2
Extremum Seeking Methods for Online Automotive Calibration

Chris Manzie, Will Moase, Rohan Shekhar, Alireza Mohammadi, Dragan Nesic and Ying Tan

Abstract The automotive calibration process is becoming increasingly difficult as the degrees of freedom in modern engines rises with the number of actuators. This is coupled with the desire to utilise alternative fuels to gasoline and diesel for the promise of lower CO_2 levels in transportation. However, the range of fuel blends also leads to variability in the combustion properties, requiring additional sensing and calibration effort for the engine control unit (ECU). Shifting some of the calibration effort online whereby the engine controller adjusts its operation to account for the current operating conditions may be an effective alternative if the performance of the controller can be guaranteed within some performance characteristics. This tutorial chapter summarises recent developments in extremum seeking control, and investigates the potential of these methods to address some of the complexity in developing fuel-flexible controllers for automotive powertrains.

2.1 Introduction

Reciprocating engines are used in transportation and stationary power generation, with diesel and gasoline representing the vast majority of the fuels used. Their environmental impact is observable in the fact that the Australian transport sector contributes approximately 15 % of national CO_2 equivalent emissions [20], while this ratio is slightly higher in the EU and US at 17.5 and 22 % respectively. Meanwhile, over the period 1990–2007 the relative cost of oil has also risen nearly 300 % [33].

C. Manzie (✉) · W. Moase · R. Shekhar · A. Mohammadi
Department of Mechanical Engineering, The University of Melbourne, Victoria, Australia
e-mail: manziec@unimelb.edu.au

D. Nesic · Y. Tan
Department of Electrical and Electronic Engineering, The University of Melbourne, Victoria, Australia

H. Waschl et al. (eds.), *Optimization and Optimal Control in Automotive Systems*, Lecture Notes in Control and Information Sciences 455,
DOI: 10.1007/978-3-319-05371-4_2,

The environmental impact of petroleum fuels has led to substantial consideration and investigation of lower CO_2 emitting alternatives. Regional dependencies dictate that the best option from a fuel security and cost perspective are not unique with the possible options including liquified petroleum gas, compressed natural gas and various levels of ethanol blending with gasoline.

While the concern over the environmental ramifications of exhaust emissions has been well publicised, the public health implications of emissions are only just coming to light. A study by the Californian Air Resources Board [5] estimated 9,000 premature deaths during 2007 in California alone are attributable to particulate matter of diameter less that 2.5 microns. By way of comparison, natural gas has less than half the particulate matter of diesel [23], and liquefied petroleum gas (LPG) has 70 % fewer particulate emissions than gasoline [4].

The downside of both these and other alternative fuels, however, is that in unrefined form their composition is variable. Consequently, subsequent operation can vary markedly, for example a 20 % change in fuel consumption was observed across a range of typical CNG blends in [10], while LPG can vary from propane-butane ratios of 25:75–100:1, with emissions performance significantly impacted [24].

From the engine control systems perspective, the challenge of changing composition is reflected in Fig. 2.1. In this figure, the torque produced from an internal combustion engine for spark sweeps on two CNG blends at a close to idle operating condition are presented. Here, an incorrect (fixed) assumption on fuel composition would lead to an incorrect MBT estimate used by the engine controller—leading to efficiency degradation and possible increased coefficient of variation of indicated mean effective pressure. The same scenario of lost optimality applies for other engine inputs.

While this approach focuses on the immediate penalty associated with changing fuel composition, the presence of hierarchical control algorithms in many of the more complex powertrains can also lead to performance and efficiency degradation if the composition is incorrectly modelled. One such example is investigated in [13], where a turbocharged flex fuel engine is used in a hybrid power train with an optimal Equivalent fuel Consumption Minimisation Strategy (ECMS) controller based on Pontryagin's Minimum Principle.

Figure 2.2 shows the fuel consumption maps mapped using E5 and E85 fuels for the test engine. In this instance, it was found that incorrect assumptions of the fuel consumption could lead to fuel efficiency degradation of the hybrid vehicle of up to 30 % relative to the best possible performance obtained when the fuel map was known perfectly and available to the ECMS-based hybrid power train controller.

For fixed fuel operation, the traditional approach to engine control is to apply a look up table approach whereby the inputs are predetermined for each engine operating point using a lengthy calibration procedure. While many proposed engine control approaches use dynamic engine models in the controller [22, 27], they typically maintain look up tables to capture properties relating to in-cylinder dynamics such as indicated efficiency. These multidimensional surfaces are obtained during a separate calibration procedure. In both situations, if the fuel composition varies from that

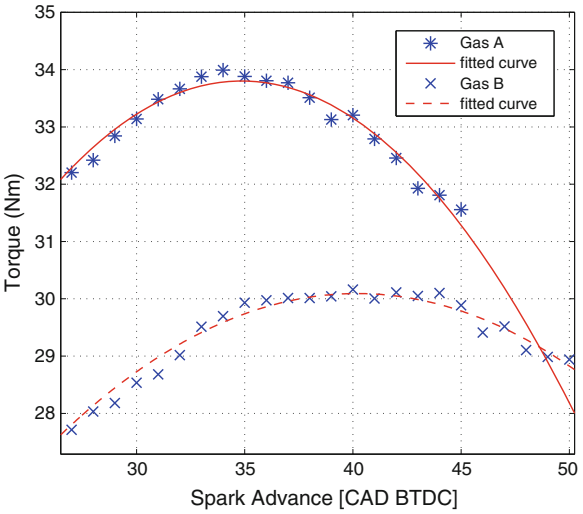

Fig. 2.1 Result of open loop spark sweeps with *Gas A* (pure methane) and *Gas B* (80 % methane, 9 % CO_2, 8.5 % N_2, 2 % ethane and 0.5 % propane) at 1,500 rpm and low load

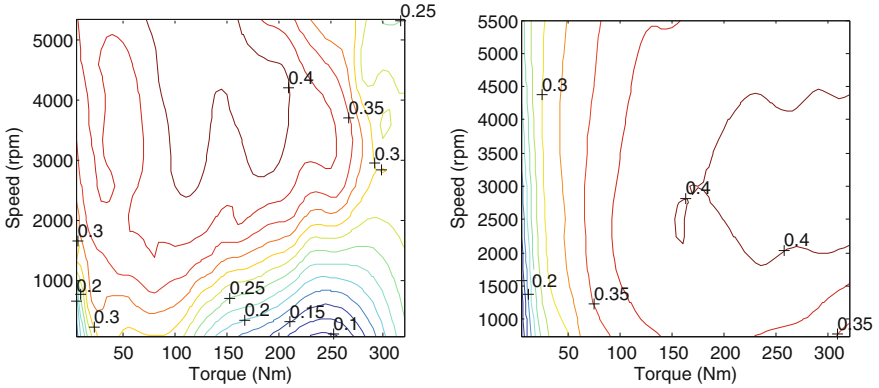

Fig. 2.2 Engine efficiency maps for a flex fuel engine running with (*left*) E05 and (*right*) E85 fuel

used during the calibration, the engine controller performs suboptimally and overall engine performance may degrade.

As a consequence, it would appear there is a need to implement some form of online optimisation to maximise the benefits promised by alternative fuels. However, the inclusion of any such adaptive capability must be in conjunction with rigorous guarantees on the performance of the closed loop system. With this in mind, recent developments in extremum seeking methods appear a good potential solution candidate, and three main categories of extremum seeking algorithms are reviewed in the subsequent section.

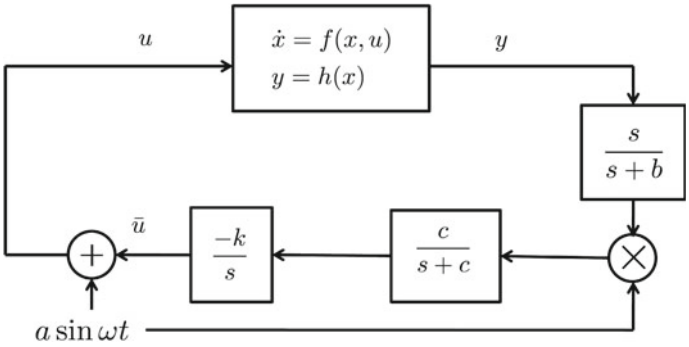

Fig. 2.3 Basic SISO extremum seeking scheme exhibiting sinusoidal perturbation to plant input, with high and low pass filters either side of demodulation step

This is then followed by a discussion of some of the automotive implementations of extremum seeking algorithms currently reported in the literature, as well as an outline of future possibilities for future research directions from both a theoretical and application based perspective.

2.2 Review of Extremum Seeking

The first known examples of extremum seeking techniques date back to 1922 [12], with several practical examples seen up until the 1950s, however the lack of formal proofs and performance guarantees led to the approach being largely set aside of several decades. This changed around the turn of the century with the development of local stability results in [11] for the basic extremum seeker shown in Fig. 2.3.

This approach essentially uses a sinusoidal perturbation to perturb the input to a dynamic plant with output y. The output is high pass filtered to remove any DC offset, before being multiplied by the dither to demodulate the gradient estimate. The gradient information can now be isolated by low pass filtering to remove all components of the plant output that are harmonics of the dither frequency. The resulting gradient estimate is then used in a gradient descent algorithm to push the plant towards its minimum. Provided the plant has a smooth output function $h(x)$ to which the output converges uniquely then semi-global practical stability is achieved with appropriate tuning of the parameters a, b, c, k and ω.

Following these initial results, many implementations of extremum seeking techniques have followed and further refinements of the theoretical foundations have been made. A comprehensive review of both the theoretical developments and applications of extremum seeking over the period 1922–2010 is provided in [30].

The extremum seeking literature can now be broadly classified into three groups: black-box approaches; grey-box approaches; and sampled data approaches. These

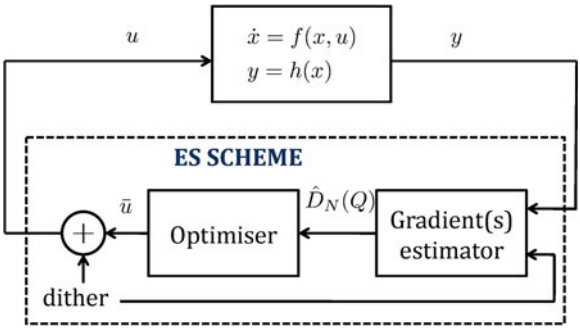

Fig. 2.4 Generalised *black* box extremum seeking framework

have different implementations and subsystem requirements which will be discussed in the following sections.

2.2.1 Black-Box Extremum Seeking

A guiding principle of the basic extremum seeking algorithm outlined above is that no model information about the plant is required, leading to it often being referred to as a black box scheme. Other approaches reported in the literature have considered alternative components in place of the filters and gradient descent in Fig. 2.3, with the essence of the majority of these black box approaches captured in Fig. 2.4, which shows the dynamic plant connected to a gradient estimator, and finally the input to the plant updated through an appropriate optimisation algorithm.

Although more formally stated in [18], the following requirements are placed on the components of Fig. 2.4 in a general setting.

Plant: The plant dynamics, $f(x,u)$ have an asymptotically stable equilibrium described for each plant input u by the surface $x = l(u)$. The input–output map of the plant at equilibrium $Q(u) := h(l(u))$ is continuous and has a unique global maximum, u^*.

Gradient estimator: Consider the first N-derivatives of $Q(u)$ as represented in the vector $D_N(Q)$, i.e.:

$$D_N(Q) := \left[\frac{dQ}{du}, \ldots, \frac{d^N Q}{du^N}\right]^T \tag{2.1}$$

The gradient estimator and dither signal must contains sufficient excitation of the plant to provide sufficiently accurate estimation of $D_N(Q)$ over a finite time interval. The dynamics of the gradient estimator may be represented as:

$$\dot{\hat{D}}_N(Q) = \varepsilon_1 F_1(\hat{D}_N(Q), P, y) \tag{2.2}$$

$$\dot{P} = \varepsilon_1 F_2(P, y) \tag{2.3}$$

Here P represents the presence of potential auxiliary states in the estimator.

Unlike in the extremum seeking scheme of Fig. 2.3, the dither need not be sinusoidal, and is only necessary to ensure the first N gradients of the input–output plant map can be estimated (assuming the chosen optimiser requires N derivatives). Consequently, various dither alternatives such as square wave, triangular wave and stochastic signals have been used. As with the dither signal, numerous gradient derivative estimators have been proposed and successfully deployed, ranging from combinations of first order filters [3, 19], through to Luenberger observers [15] and Kalman filters [32]. The dynamics of the gradient estimator are controlled through the tuning parameter ε_1, representing for example the cut-off frequency of the high pass filter or the gain used by a Luenberger observer. The suitable choice of ε_1 typically delivers time scale separation of the plant and estimator dynamics.

Optimiser: Consider the continuous optimisation algorithm operating on known derivatives $D_N(Q)$ of a static map $Q(z)$:

$$\dot{z} = \varepsilon_2 F_3(z, D_N(Q(z))) \tag{2.4}$$

The chosen optimisation algorithm ensures that the output of the static map $Q(z)$ converges to the optimum value, $Q(z^*)$, with some degree of robustness. Again there are many possible choices for the optimiser, ranging from the gradient descent approach shown in Fig. 2.3, to higher order optimisers such as Newton step [15] and other variants, although all typically have tunable dynamics represented by ε_2. As with the gradient estimator, the choice of ε_2 is used to ensure time scale separation, this time between the gradient estimator and the optimiser.

This decomposition of the closed loop extremum seeking scheme enables the practitioner to independently select the optimiser and gradient estimator from families of possible options satisfying the requirements stated above. The overall convergence of the system is then guaranteed by ensuring that the plant, gradient estimator and optimiser occupy different time scales (formally stated in Theorem 1 of [18]). This is achieved by selecting the gains such that the gradient estimator is sufficiently slower than the plant, and the optimiser is sufficiently slower than the gradient estimator to ensure time scale separation—therefore enabling the plant to be 'seen' as a static map by the gradient estimator, and both components to be 'seen' as static by the optimiser.

There is a tradeoff to be balanced in selecting the gains and dither, as smaller values yield slower convergence but guarantee the convergence of the output will be to a smaller vicinity of the optimum of the static map, $Q(u)$.

The generality of the framework presented above is useful in guaranteeing convergence and developing tuning rules despite very little knowledge of the plant. However, one potential drawback of this generality is the conservativeness of the result particularly in terms of convergence rate, to ensure time scale separation between

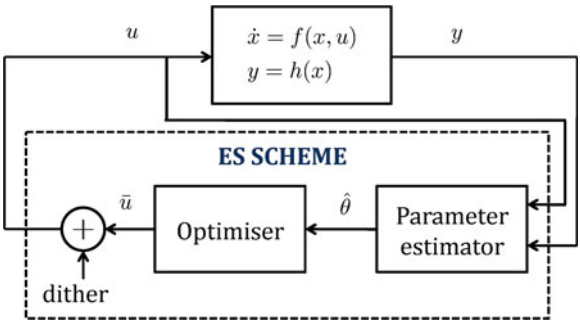

Fig. 2.5 Generalised it grey box extremum seeking framework

the major system elements. With greater specificity about the plant structure, and by utilising particular schemes for gradient estimation and optimisation, faster convergence properties can be obtained. Such approaches have been described for Wiener-Hammerstein plants [14], and principally rely on plant input and output filters to remove the need to wait for plant dynamics to settle before updating the extremum seeking output. This allows for high frequency dithers to be employed and arbitrarily fast (in the absence of noise) convergence to be achieved.

2.2.2 Grey-Box Extremum Seeking

The fast extremum seeking approaches of the previous section utilise knowledge about the plant dynamics in the design of the input and output filters. In many practical applications however, there is knowledge of the basic form of the optimisation surface, $Q(u)$, to which the dynamics converge. The utilisation of this knowledge in an extremum seeking context falls largely in the domain of the so-called grey box approaches. Here, the surface $Q(u)$, is parameterised in terms of a vector of unknown parameters, θ, i.e.:

$$Q(u,\theta) = \Psi(u)^T\theta \tag{2.5}$$

Thus, by estimating θ potentially non-local information about the surface can be obtained. In [1, 2], this approach was explored for specific instances of the parameter estimator and optimiser, and then further generalised in [16] leading to a description of the closed loop system in the form shown in Fig. 2.5.

The parallels with the generalised black box framework of Fig. 2.4 are clear, and there exist similar requirements on the plant and optimiser in the grey box scheme, although the following requirement for the parameter estimator replaces that for the gradient estimator given above.

Parameter estimator: The parameter estimator can be represented in the general form as states directly relevant to the parameter estimates and additional states within the parameter estimator, i.e.:

$$\dot{\hat{\theta}} = \varepsilon_1 G_1(\hat{\theta}, P, y, u) \tag{2.6}$$

$$\dot{P} = \varepsilon_1 G_2(P, y, u) \tag{2.7}$$

The parameter estimator and dither signal combination needs to contains sufficient excitation of the plant to provide estimation of the parameters within a finite time interval. A thorough analysis of a number of different parameter estimation schemes was conducted in [16], with possibilities for deployment including gradient algorithms with and without integral costs along with least squares estimation variants.

By incorporating the parameter estimator in place of the gradient estimator, the optimiser can potentially utilise differently structured optimisers that may take advantage of the estimated map, while still satisfying the time scale separation of the black box scheme. This reliance on time scale separation implies that substantial increases in convergence rates over the black box approach are not necessarily forthcoming.

With this in mind, preliminary research has been made into algorithm specific grey box approaches that lack the generality of the framework described above but may have potential along the lines of the fast black box approaches described in the previous section [26].

2.2.3 Sampled Data Approaches

The previous two categories of extremum seeking algorithms use continuous time optimisation algorithms, and consequently only draw upon the discrete time optimisation field indirectly through the time scale separation providing the optimiser can satisfy the requirements. An alternative viewpoint, drawing more directly on nonlinear programming techniques, was first presented in [31], and is illustrated in Fig. 2.6.

In this approach, the dynamic plant is treated as a system to be sampled, with a finite number of sampled plant outputs used to estimate derivatives of the static map before the control input is updated, and enabled the use of many discrete time optimisation algorithms such as Finite Differencing and Simultaneous Perturbation Stochastic Approximation (SPSA) [29]. The work was generalised further in [9], where a different style of proof was used and required the discrete time optimisation algorithm to be uniformly attractive with respect to small additive disturbances, rather than asymptotically stable as in [31]. The later approach also opens the possibility for non-gradient based global optimisation algorithms such as Piyavskii-Shubert and DIRECT to be rigorously deployed [8, 17] thereby reducing the requirement that the plant have only one global optimum—albeit at significant convergence time penalties relative to the local optimisation techniques.

As seen with the continuous extremum seeking approaches, there may be advantages in forsaking generality of the sampled data approach and focusing on a specific combination of discrete time optimiser and plant. In [28], a discrete time Hammerstien plant is subjected to an algorithm using a square wave dither with a two step

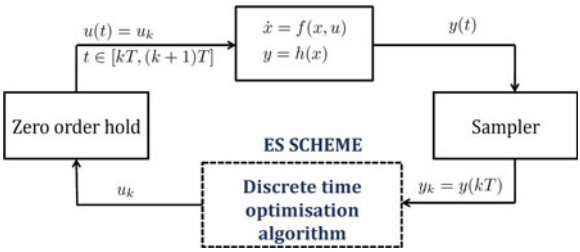

Fig. 2.6 Generalised sampled data extremum seeking framework

averaging filter with the specific nature of the system enabling LPV techniques to be used to generate an exponential stability result.

2.3 Application to Automotive Engine Calibration

One of the earliest applications of extremum seeking in the automotive calibration context was in [25], where a grey box extremum seeking architecture was designed and implemented for spark control on a gasoline spark ignition engine. The approach assumed a quadratic map between the spark angle and indicated torque, similar to Fig. 2.1. The parameters of the quadratic were then estimated using a recursive least squares estimator, although the optimiser used attempted to immediately drive the control input to the optimum level as calculated by the estimated parameters, and consequently the time scale separation required for convergence guarantees in the grey-box schemes of Sect. 2.2.2 was not present. Thus while successful results were reported, the initial conditions of the parameter estimator need to be sufficiently close to the true values for convergence to occur.

Addressing the multi-variable calibration problem from an extremum seeking perspective was explored in [21]. This approach considered a sampled data implementation of extremum seeking (as in Sect. 2.2.3), with the actuation variables of intake and exhaust valve timing along with the spark timing. From arbitrary initial conditions, the calibration process using extremum seeking was found to take around 15 min to locate the optimum, largely impacted by the multivariable nature of the problem and the noise associated with torque measurements requiring long averages of measured data.

In-service alternative fuelled engines may experience regular fuel composition changes, yet the opportunity to undertake manual recalibration is not present. The growing interest in these engines has renewed interest in online calibration. One recent implementation considered the situation for flex-fuelled engines [6] considers a ES implementation in the class of black box systems described in Sect. 2.2.1 to maximise fuel economy by adjusting the spark. This approach utilises a discrete time version of the black box approach of the form given in Fig. 2.3, with a square

wave perturbation. Unlike in [21], only the spark is changed and this single variable nature of the optimisation coupled with the fact that the optimisation problem is effectively 'hot-started' as the optimal spark will not vary significantly between different ethanol-gasoline blends means the outcome is more positive in terms of real world deployability.

In a similar vein, but with compressed natural gas blends as the fuel source, different implementations of the grey box extremum seeking framework falling under the framework of [16] were investigated as possible spark optimisation strategies. Experiments are carried out for two blended pure methane and a blended gas consisting of 80 % methane, 9 % carbon dioxide, 8.5 % nitrogen, 2 % ethane and 0.5 % propane. As with [25] and shown in Fig. 2.1, open loop tests demonstrate that a quadratic polynomial approximation seems a good representation of the data, allowing the following model to be used relating torque, τ, and spark α:

$$\tau(\alpha) = \lambda_1 \alpha^2 + \lambda_2 \alpha + \lambda_3 \tag{2.8}$$

Defining the regressor vector $\phi = [\alpha^2 \ \alpha \ 1]^T$, the grey box approach then involves the selection and tuning of appropriate parameter estimator for $\theta := [\lambda_1 \ \lambda_2 \ \lambda_3]^T$, and an optimiser to drive τ towards τ^*.

To demonstrate the flexibility afforded by the framework approach, experiments were conducted using two different estimator-optimiser combinations. The first consisted of recursive least squares parameter estimator and gradient based optimiser, while the second consisted of a gradient based parameter estimator and a Jacobian-matrix transpose optimisation metric. All parameter estimators and optimisers had previously been shown to satisfy the theoretical requirements of the grey box framework in [16], and the tuned algorithms are repeated below in (2.9)–(2.13). The discrete nature of the presented algorithms reflects an emulation of the continuous time versions of (2.6)–(2.7) and (2.4).

Gradient-based parameter estimator after tuning:

$$\hat{\theta}_{k+1} = \hat{\theta}_k - [0.002 \ \ 0.05 \ \ 1]^T (\tau_k - \phi_k^T \hat{\theta}_k) \tag{2.9}$$

Recursive least squares parameter estimator after tuning:

$$\hat{\theta}_{k+1} = \hat{\theta}_k + P_k \phi_k (\tau_k - \phi_k^T \hat{\theta}_k) \tag{2.10}$$

$$P_{k+1} = P_k + (0.9 P_k - P_k \phi_k^T \phi_k P_k) \tag{2.11}$$

Gradient based optimiser after tuning:

$$\hat{\alpha}^*_{k+1} = \hat{\alpha}^*_k + 10(2\hat{a}_k \hat{\alpha}^*_k + \hat{b}_k) \tag{2.12}$$

Jacobian matrix transpose optimiser after tuning:

$$\hat{\alpha}^*_{k+1} = \hat{\alpha^*_k} - 75\hat{a}_k (2\hat{a}_k \hat{\alpha}^*_k + \hat{b}_k) \tag{2.13}$$

The applied spark advance is then the current estimate of the optimal spark advance, $\hat{\alpha}_k^*$, perturbed by a sinusoidal dither of amplitude one crank angle degree, i.e.:

$$\alpha_k = \hat{\alpha}_k^* + \sin(0.1kT) \tag{2.14}$$

All experiments to test these algorithms were conducted in the test cell of the ACART Laboratory at the University of Melbourne. The engine tested a six cylinder 4L Ford Falcon BF MY2006 gasoline engine which is converted to operate with natural gas.

In order to keep the speed and load of the engine constant, an eddy current dynamometer is used which can only work as a brake and is not capable of motoring the engine. The air-fuel ratio was maintained at an approximately stoichiometric condition by adjusting the injection duration with feedback from a wide-band exhaust oxygen gas sensor. The proposed algorithms were implemented in MATLAB. The output of the MATLAB program were sent in realtime directly to the engine control unit (ECU) via ATI Vision software, thereby adapting the stored calibration. The delays in communication between the different software programs were measured at approximately 6 ms, which was considered negligible in the context of this application. Feedback torque was obtained through measurements from a load cell on the dynamometer, although in the future could be replaced by in-cylinder pressure sensors and appropriate combustion analysis. The torque measurement was averaged over a period of three seconds to minimize the effects of combustion variability and measurement noise. The sample rate used by the controller was set nominally to 5 s so as to be longer than the torque measurement time.

The engine control unit was initially calibrated using the blended methane gas, leading to an initial estimate of MBT at approximately 40° BTDC. The actual fuel used in the engine was pure methane, and consequently the extremum seeking controllers were required to adapt the spark to find the new MBT spark, which lies at approximately 33° BTDC, although may vary slightly with engine temperature. The adapted spark and resulting engine torque for each of the two extremum seeking combinations are shown in Figs. 2.7 and 2.8.

In both instances, (although not shown) the parameter estimates also converge to a vicinity of the 'true' values, and the spark converges to a close vicinity of the optimum. To quantify the gains in efficiency the incorporation of these extremum seeking approaches strategies may provide, the fuel flow rate of the engine running with the initial spark advance at the specified operating point was compared to fuel flow rate after convergence of the spark to the optimal value. This latter value was corrected to allow for the torque difference although in practice this could be achieved through modification to the throttle angle. Consequently it was found that the fuel economy improved by approximately 3 % at this static operating condition.

To further demonstrate the flexibility of viewing extremum seeking as a framework approach, a sampled data approach is also presented for the same engine. In this approach, an ES scheme using a simple alternating dither signal $a(-1)^k$ is added to the current estimate for the optimising value of the system input, and used as the applied spark in place of (2.14). The resulting torque (after the two second averaging)

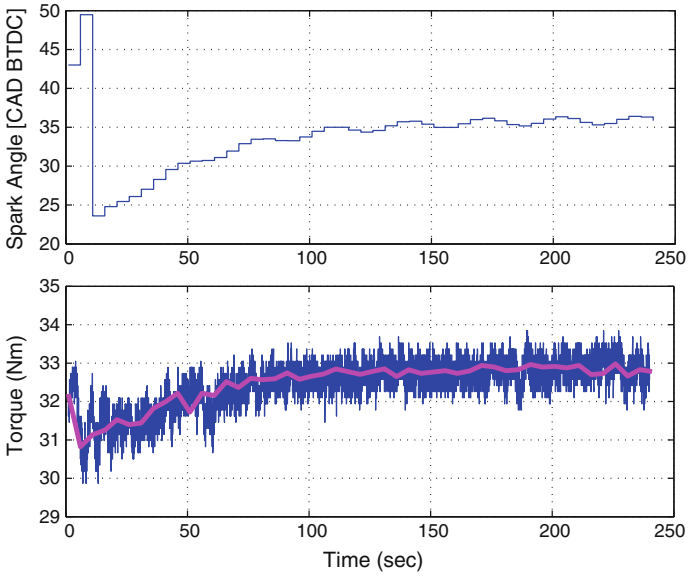

Fig. 2.7 *Grey* box convergence for a recursive least squares parameter estimator and gradient based optimiser (*top*) spark advance (*bottom*) measured and 2 s averaged engine torques

is multiplied by the signal $(-1)^k$ and passed through a two-step moving-average FIR filter and discrete-time integrator. This advances the estimate for the optimising value according to an approximate gradient ascent law, based on a two-point central difference approximation applied to the engine spark-to-torque mapping. The entire closed loop scheme is represented by the block diagram shown in Fig. 2.9.

Implementing this sampled data extremum seeking approach on the same engine set up as described previously, with an initial estimate of MBT spark of 22° leads to the results shown in Fig. 2.10. As previously observed for the grey box approaches, convergence to the vicinity of the optimum spark and torque occurs and there is a subsequent improvement in fuel economy of approximately 3 % at this operating point relative to the case of no adaptation of the spark.

The convergence speed of the algorithms tested in this section warrants discussion. As shown in Figs. 2.7–2.10, the schemes take of order 100 s to converge to the optimum at a fixed operating condition. On its own, this convergence time is not of significant concern as the rate of change of fuel composition is much slower thereby allowing even a 100 s transient to be deemed negligible if steady state operation is considered.

During transient engine operation, such as might be considered during urban driving, it is however unlikely that the engine will remain at a constant, non-idle operating condition for periods of this duration. The convergence rate is a consequence of the nature of the time scale separation requirement of the plant, estimator and optimiser for the extremum seeking framework-based theory, which is

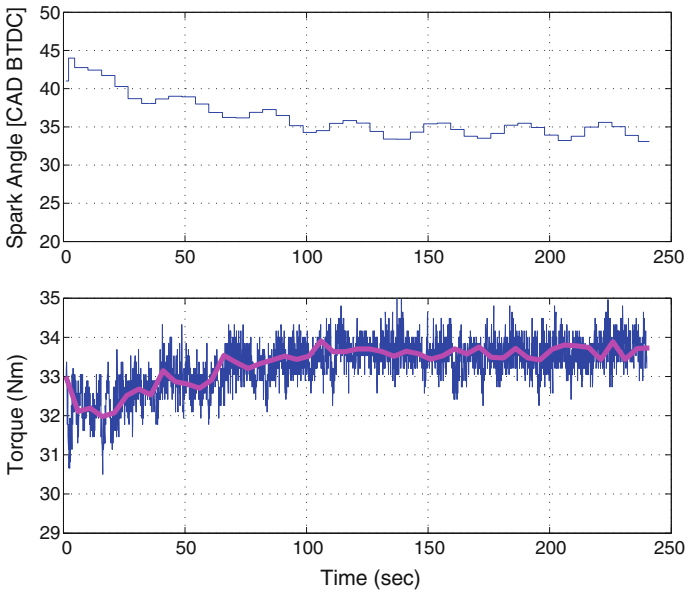

Fig. 2.8 *Grey* box convergence for a gradient based parameter estimator and Jacobian matrix transpose (*top*) spark advance (*bottom*) measured and 2 s averaged engine torques

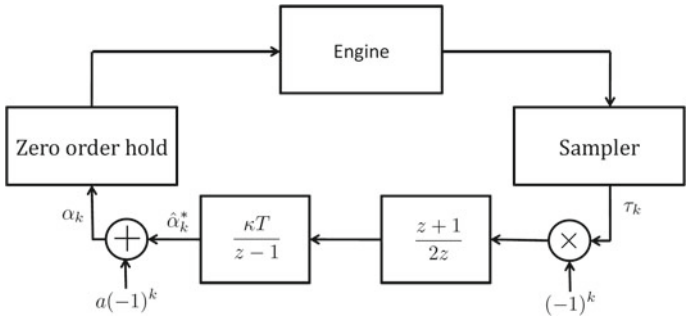

Fig. 2.9 Proposed sampled data extremum seeking approach for optimal spark estimation on CNG engine

principally centred on guaranteeing convergence using very relaxed requirements on the components of the closed loop scheme. By being more restrictive in the selection of these components, the tuning requirements can be modified and the convergence rate can potentially be sped up using the faster extremum seeking approaches in the vein of [14].

Finally, for the purposes of demonstration of the extremum seeking techniques, brake torque has been directly measured and used as the feedback to be optimised in these experiments. Such a measurement is clearly not directly available in an

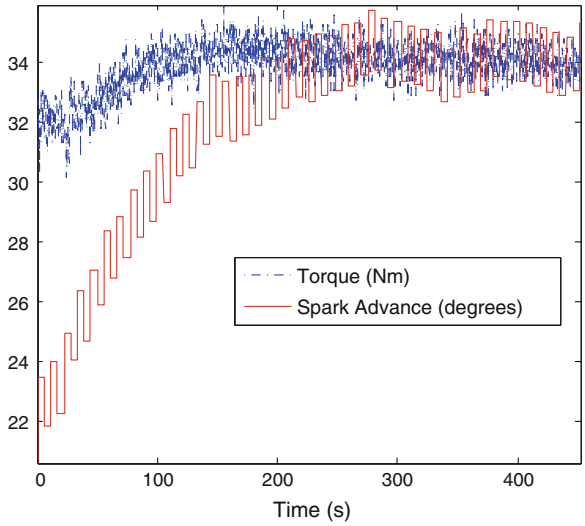

Fig. 2.10 Spark and torque progression under the proposed sampled data extremum seeking approach with $a = 1^\circ$

on-road application, and so surrogate measurements must be employed depending on the available sensor set.

2.4 Incorporation of Constraints

Not discussed in the methodology so far is the issue of constraint management. For input constraints, if the plant inputs, $\bar{u}$, are required to lie within a set, U_c, the optimiser can explicitly take this into account by projecting the new optimiser output, $\bar{u}_{proj}$ onto the Pontryagin difference of the constraint set and the dither set, D i.e.:

$$U_c \sim D \triangleq \{\bar{u} \in R^n \mid \bar{u} + d \in U_c, \forall d \in D\} \tag{2.15}$$

$$\bar{u}_{proj} = \text{proj}(\bar{u}, U_c \sim D) \tag{2.16}$$

This ensures the dither is still able to persistently excite the system, even approaching the constraint boundary, and the gradient or parameter estimates in the black or grey box schemes are maintained.

In the context of the engine calibration problem, this might mean for example the physical actuator limits are captured so that, for example, the spark is constrained to occur within the compression stroke of that cylinder. These types of constraints are rigorously enforceable.

On the other hand, state constraints are not so easily dealt with as generally there is no concept of 'state' in the model used in an extremum seeking controller. In

this case, an approximate solution is that the state constraints must be mapped to input constraints, so that U_c in (2.15)–(2.16) becomes time varying and most likely requires online estimation.

Again in the context of the online calibration problem, the spark timing in a natural gas engine is often constrained by knock limitations. The occurrence of knock is related to the fuel composition, which can be viewed as an internal state and is clearly unknown from the problem definition. Knock detection algorithms (see e.g. [7] and the references within) can be used to continually estimate the knock limit on spark advance, which may then be used to update the constraint set U_c.

2.5 Summary and Future Opportunities

The recent development of extremum seeking frameworks has delivered considerable flexibility into the deployment of different algorithms to achieve convergence to optimal performance in many applications. To the automotive community, this appears to be highly relevant as the industry continues a progression towards alternative fuels exhibiting variable composition, thereby necessitating some form of closed loop calibration being conducted during regular vehicle operation.

There remain a number of theoretical challenges and opportunities for research in extremum seeking algorithms. These include research into increasing the convergence rate without unduly compromising the region of attraction; dealing with map uncertainty in grey box frameworks; handling state constraints within the various frameworks; and identifying when certain frameworks might lead to better closed loop performance.

Similarly, there are also application-centric issues for automotive calibration including the deployment of the algorithms in transient driving conditions; implementing some of the novel theoretical developments promising faster convergence for online multivariable calibration; consideration of emissions in the cost function; and the integration with model based techniques for faster offline calibration particularly in highly actuated engines.

Acknowledgments The support of the Advanced Centre for Automotive Research and Testing (ACART, http://www.acart.com.au) and the Australian Research Council (ARC) is gratefully acknowledged.

References

1. Adetola V, DeHaan D, Guay M (2009) Adaptive model predictive control of constrained nonlinear systems. Syst Control Lett 58:320–326
2. Adetola V, Guay M (2006) Adaptive output feedback extremum seeking receding horizon control of linear systems. J Process Control 16:521–533
3. Ariyur KB, Krstic M (2003) Real time optimisation by extremum seeking control. Wiley, New York

4. Beer T, Grant T, Williams D, Watson H (2002) Fuel-cycle greenhouse gas emissions from alternative fuels in australian heavy vehicles. Atmos Environ 36:753–763
5. Californian Air Resources Board. Estimate of Premature Deaths Associated with Fine Particle Pollution (PM2.5) in California Using a U.S. Environmental Protection Agency, Methodology. August, 2010
6. Hellström E, Lee D, Jiang L, Stefanopoulou AG, Yilmaz H (2013) On-board calibration of spark timing by extremum seeking for flex-fuel engines. IEEE Trans Control Syst Technol 21(6):2273–2279
7. Jones JCP, Frey J, Muske KR, Scholl DJ (2010) A cumulative-summation-based stochastic knock controller. In: Proceedings of the institution of mechanical engineers part D: journal of automobile engineering 224:969–983
8. Khong SZ, Nesic D, Manzie C, Tan Y (2013) Multidimensional global extremum seeking via the direct optimisation algorithm. Automatica 49(7):1970–1978
9. Khong SZ, Nesic D, Tan Y, Manzie C (2013) Unified frameworks for sampled-data extremum seeking control: global optimisation and multi-unit systems. Automatica 49(9):2720–2733
10. Kim K, Kim H, Kim B, Lee K (2009) Effet de la composition du gaz naturel sur les performances d'un moteur GNC. Oil Gas Sci Technol Rev IFP 64(2):199–206
11. Krstic M, Wang H-H (2000) Stability of extremum seeking feedback for general nonlinear dynamic systems. Automatica 36:595–601
12. Leblanc M (1922) Sur lõelectrification des chemins de fer au moyen de courants alternatifs de frequence elevee. Revue Generale de lõElectricite
13. Manzie C, Grondin O, Sciarretta A, Zito G (2013) Robustness of ECMS-based optimal control in parallel hybrid vehicles. In: 7th IFAC symposium on advances in automotive, control
14. Moase W, Manzie C (2012) Fast extremum—seeking for Wiener-Hammerstein plants. Automatica 48:2433–2443
15. Moase W, Manzie C, Brear M (2010) Newton—like extremum—seeking for the control of thermoacoustic instability. IEEE Trans on Autom Control 55:2094–2105
16. Nesic D, Mohammadi A, Manzie C (2013) A framework for extremum seeking control of systems with parameter uncertainties. IEEE Trans Autom Control 58:435–448
17. Nesic D, Nguyen T, Tan Y, Manzie C (2013) A non-gradient approach to global extremum seeking: an adaptation of the Shubert algorithm. Automatica 49(3):809–815
18. Nesic D, Tan Y, Manzie C, Mohammadi A, Moase W (2012) A unifying framework for analysis and design of extremum seeking controllers. In: 24th Chinese decision and control conference (CCDC)
19. Nesic D, Tan Y, Moase W, Manzie C (2010) A unifying approach to extremum seeking: adaptive schemes based on derivative estimation. In: IEEE conference on decision and control
20. Australian Government Department of Climate Change (2009) National greenhouse gas inventory. http://www.climatechange.gov.au/inventory
21. Popovic D, Jankovic M, Magner S, Teel A (2006) Extremum seeking methods for optimization of variable cam timing engine operation. IEEE Trans Control Syst Technol 14:398–407
22. Del Re L, Allgöwer F, Glielmo L, Guardiola C, Kolmanovsky I (eds) (2010) Automotive model predictive control: models, methods and applications. Springer, Heidelberg
23. Ristovski ZD, Jayaratne ER, Morawska L, Ayoko GA, Liml M (2005) Particle and carbon dioxide emissions from passenger vehicles operating on unleaded petrol and LPG fuel. Sci Total Environ 345:93–98
24. Saleh HE (2008) Effect of variation in LPG composition on emissions and performance in a dual fuel diesel engine. Fuel 87(13–14):3031–3039
25. Scotson P, Wellstead PE (1990) Self-tuning optimization of spark ignition automotive engines. IEEE Control Syst Mag 3:94–101
26. Sharafi J, Moase W, Shekhar RC, Manzie C (2013) Fast model-based extremum seeking on hammerstein plants. In: IEEE conference on decision and control
27. Sharma R, Nesic D, Manzie C (2013) Sampled data model predictive idle speed control of ultra-lean burn hydrogen engines. IEEE Trans Control Syst Technol 21:538–545

28. Shekhar RC, Moase W, Manzie C (2013) Semi-global stability analysis of a discrete-time extremum-seeking scheme using LDI methods. In: IEEE conference on decision and control
29. Spall J (2000) Adaptive stochastic approximation by the simultaneous perturbation method. IEEE Trans Autom Control 45:1839–1844
30. Tan Y, Moase WH, Manzie C, Nesic D, Mareels IMY (2010) Extremum seeking from 1922 to 2010. In: 29th Chinese control conference, pp 14–26
31. Teel AR, Popovic D (2001) Solving smooth and nonsmoooth multivariable extremum seeking problems by the methods of nonlinear programming. In: Proceedings of the American control conference, pp 2394–2399
32. Wiederhold O, King R, Noack B, Neuhaus L, Neise W, Enghardt L, Swoboda M (2009) Extensions of extremum—seeking control to improve the aerodynamic performance of axial turbomachines. In: 39th AIAA fluid dynamics conference
33. WTRG-Economics Oil price history and analysis (2013). http://www.wtrg.com/prices.htm

http://www.springer.com/978-3-319-05370-7

Optimization and Optimal Control in Automotive Systems

Waschl, H.; Kolmanovsky, I.; Steinbuch, M.; del Re, L. (Eds.)

2014, XX, 326 p. 157 illus., 103 illus. in color., Softcover
ISBN: 978-3-319-05370-7